Supplementary Information

Highly Efficient Green Organic Light-Emitting Diodes Containing Luminescent Tetrahedral Copper(I) Complexes

Satoshi Igawa,[a,b] Masashi Hashimoto,[a,b] Isao Kawata,[a,c] Masataka Yashima,[a,b] Mikio Hoshino[a] and Masahisa Osawa*[,a]

[a]*Luminescent Materials Laboratory, RIKEN, Hirosawa 2-1, Wako-Shi, 351-0198, Japan.*
[b]*Device Technology Development Headquartersc, Ohta-ku, Tokyo 146-8501, Japan.*
[c]*Analysis Technology Center, Canon Incorporated, Ohta-ku, Tokyo 146-8501, Japan.*

Contents

Experimental Details

1. Synthetic Details

Materials. 1,2-Bis(dichlorophosphino)benzene and magnesium were obtained from Wako Pure Chemical Industries, Ltd. 3,5-Difluorophenylmagnesium bromide and bromo(dimethylsulfide)copper(I) ($CuBr{\cdot}SMe_2$) were purchased from Sigma-Aldrich. 1-Bromo-3,5-bistrifluoromethylbenzene was obtained from TCI. Co., Ltd. Iodine was purchased from Kanto Chemical Co., Inc. Di-[4-(N,N-ditolyl-amino)-phenyl]cyclohexane (TAPC), 1,3-bis(carbazol-9-yl)benzene (mCP), and tris(2,4,6-trimethyl-3-(pyridine-3-yl)phenyl)borane (3TPYMB) were purchased from Lumitec Corp. Potassium diphenylbis(pyrazol-1-yl)borate ($KBpz_2ph_2$) and $[(dppb)CuBr]_2$ were prepared according to literature procedures.[1,2]

Synthesis of dppb-F. A solution of 3,5-difluorophenyl magnesium bromide in THF (0.5M, 50 mL, 25 mmol) was added dropwise to a solution of 1,2-bis(dichlorophosphino)benzene (1.0 g, 3.57 mol) in THF (20 mL) at 0 ºC. The reaction mixture was stirred at room temperature for 4 h. A solution of saturated aqueous NH_4Cl (100 mL) was added to the reaction mixture, and extracted with CH_2Cl_2 (3 × 60 mL). The combined organic extracts were washed with saturated aqueous NaCl (150 mL) and dried over $MgSO_4$. The drying agent was removed by filtration, and the solvent was removed *in vacuo* to give a pale yellow oil. The residue was purified by column chromatography on silica gel (*n*-hexane/CH_2Cl_2, 2:1) to afford dppb-F (933 mg, 47%) as a colorless solid. ^{1}H NMR (500 MHz, CD_2Cl_2, 300 K): δ 6.69 (m, 8H), 6.79 (m, 4H), 7.11 (m, 4H), 7.43 (m, 2H); ^{13}C NMR (125 MHz, CD_2Cl_2, 300 K): δ 104.89, (t, $J_{C\text{-}P}$ = 25.2 Hz), 116.41 (m), 130.82, 134.52 (t, $J_{C\text{-}P}$ = 3.4 Hz), 140.26 (m), 141.54 (t, $J_{C\text{-}P}$ = 10.9 Hz), 162.21 (m), 164.12 (m); ^{19}F NMR (377 MHz, CD_2Cl_2, 300 K): δ -111.66; ^{31}P {^{1}H} NMR (202 MHz, CD_2Cl_2, 300 K): δ -9.60. Anal. calcd. for $C_{30}H_{16}F_8P_2$ (%): C, 61.03; H, 2.73. Found: C, 61.29; H, 2.81.

Synthesis of dppb-CF_3. A solution of 3,5-bis(trifluoromethyl)phenyl magnesium bromide was prepared from magnesium (3.0 g, 125 mmol) and 1-bromo-3,5-bis(trifluoromethyl)benzene (36.5 g, 125 mmol) in THF (100 mL), and then cooled to 0 ºC. A solution of 1,2-bis(dichlorophosphino)benzene (5.0 g, 16.8 mol) in THF (20 mL) was added dropwise to the solution of 3,5-bis(trifluoromethyl)phenyl magnesium bromide. The reaction mixture was stirred at room temperature for 4 h. A solution of saturated aqueous NH_4Cl (100 mL) was added to the reaction mixture, and then the mixture was extracted with CH_2Cl_2 (3 × 80 mL). The combined organic extracts were washed with saturated aqueous NaCl (150 mL) and dried over $MgSO_4$. The drying agent was removed by filtration, and the solvent was removed *in vacuo* to give a pale yellow oil. The residue was purified by column chromatography on silica gel (*n*-hexane/CH_2Cl_2, 2:1) to

afford dppb-CF_3 (12.4 g, 74%) as a colorless solid. ^{1}H NMR (500 MHz, CD_2Cl_2, 300 K): δ 7.23 (m, 2H), 7.54 (m, 2H), 7.03 (m, 8H), 7.90 (m, 4H); ^{13}C NMR (125 MHz, CD_2Cl_2, 300 K): δ 122.93 (q, $J_{C\text{-}F}$ = 271.5 Hz), 123.87, 131.93, 132.40 (qt, $J_{C\text{-}F}$ = 33.7, $J_{C\text{-}P}$ = 3.2 Hz), 133.50 (2C), 134.73 (t, $J_{C\text{-}P}$ = 3.1 Hz), 135.09 (t, $J_{C\text{-}P}$ = 5.5 Hz), 140.41 (t, $J_{C\text{-}P}$ = 11.4 Hz); ^{19}F NMR (377 MHz, CD_2Cl_2, 300 K): δ -65.92. ^{31}P {^{1}H} NMR (202 MHz, CD_2Cl_2, 300 K) δ -11.46. Anal. calcd. for $C_{38}H_{16}F_{24}P_2$ (%): C, 46.08; H, 1.63. Found: C, 46.42; H, 1.89.

Cu(dppb)(pz_2Bph_2) (1). $KBpz_2ph_2$ (338 mg, 0.5 mmol) was added to a solution of $[(dppb)CuBr]_2$ (236 mg, 0.2 mmol) in THF (15 mL). The reaction mixture was stirred at room temperature for 2 h. The reaction mixture was filtered, and the solvent was removed *in vacuo* to give a pale yellow powder. The residue was purified by recrystallization from CH_2Cl_2 / *n*-hexane to give yellow crystals (268 mg, 83%). ^{1}H NMR (500 MHz, CD_2Cl_2, 300 K) δ 6.02 (t, 2H, *J* = 2.0 Hz), 6.70 (m, 4H), 6.82 (t, 4H, *J* = 7.0 Hz), 6.87 (m, 2H), 6.89 (m, 2H), 7.02-7.06 (m, 8H), 7.23 (m, 10H), 7.32 (t, 4H, *J* = 7.0 Hz), 7.41-7.46 (m, 4H); ^{13}C NMR (125 MHz, CD_2Cl_2, 300 K) δ 102.72, 125.49, 126.68, 128.42 (t, $J_{C\text{-}P}$ = 4.4 Hz), 129.20, 130.39, 133.17 (t, $J_{C\text{-}P}$ = 8.2 Hz), 133.71, 134.14 (t, $J_{C\text{-}P}$ = 14.2 Hz), 134.85 (t, $J_{C\text{-}P}$ = 3.9 Hz), 136.98, 141.63, 143.24 (t, $J_{C\text{-}P}$ = 32.5 Hz); ^{31}P {^{1}H} NMR (202 MHz, CD_2Cl_2, 300 K) δ –8.71.Anal. calcd. for $C_{48}H_{40}BCuN_4P_2$ (%): C, 71.25; H, 4.98; N, 6.92. Found: C, 71.03; H, 5.10; N, 6.72.

Cu(dppb-F)(pz_2Bph_2) (2). A solution of dppb-F (354 mg, 0.6 mmol) in THF (20 mL) was added dropwise to the a solution of $CuBr{\cdot}SMe_2$ (124 mg, 0.6 mmol) in THF (10 mL). The reaction mixture was stirred at room temperature for 1 h. A solution of $KBpz_2ph_2$ (146 mg, 0.73 mmol) in THF (10 mL) was added to the reaction mixture, and then it was stirred at room temperature for 1 h. The solvent was removed from the reaction mixture *in vacuo* to give a pale yellow oil. The residue was purified by recrystallization from CH_2Cl_2 / *n*-hexane to give yellow crystals (406 mg, 71%). ^{1}H NMR (500 MHz, CD_2Cl_2, 300 K): δ 6.16 (m, 2H), 6.59 (m, 8H), 6.68 (m, 4H), 6.86 (m, 4H), 6.92 (m, 6H), 6.97 (m, 2H), 7.33 (m, 2H), 7.44 (m, 2H), 7.61 (m, 2H); ^{13}C NMR (125 MHz, CD_2Cl_2, 300 K): δ 103.36, 105.74 (t, $J_{C\text{-}P}$= 25.1 Hz), 124.74, 115.79 (dt, $J_{C\text{-}F}$ = 26.0, $J_{C\text{-}P}$ = 8.7 Hz), 125.68, 126.87, 132.10, 133.47, 135.01 (t, $J_{C\text{-}P}$ = 3.6 Hz), 136.55 (m), 137.85, 140.71 (t, $J_{C\text{-}P}$ = 33.2 Hz), 141.51, 161.13 (dt, $J_{C\text{-}F}$ = 11.8, $J_{C\text{-}P}$ = 6.6 Hz) , 164.13 (dt, $J_{C\text{-}F}$ = 11.8, $J_{C\text{-}P}$ = 6.6 Hz); ^{19}F NMR (377 MHz, CD_2Cl_2, 300 K): δ -111.47; ^{31}P {^{1}H} NMR (202 MHz, CD_2Cl_2, 300 K) δ -7.98. Anal. calcd. for $C_{48}H_{32}BCuF_8N_4P_2$ (%): C, 60.49; H, 3.38; N, 5.88. Found: C, 60.71; H, 3.27; N, 5.69.

[Cu(dppb-CF_3)(pz_2Bph_2) (3). A solution of dppb-CF_3 (600 mg, 0.6 mmol) in THF (20 mL) was added dropwise to a solution of $CuBr{\cdot}SMe_2$ (124 mg, 0.6 mmol) in THF (10 mL). The reaction mixture was stirred at room temperature for 1 h. A solution of $KBpz_2ph_2$ (146 mg, 0.73 mmol) in

THF (10 mL) was added to the reaction mixture, which was then stirred at room temperature for 1 h. The solvent was removed *in vacuo* to give a pale yellow oil, which was purified by recrystallization from CH_2Cl_2 / *n*-hexane to give yellow crystals (416 mg, 51%). ^{1}H NMR (500 MHz, CD_2Cl_2, 300 K): δ 6.24 (t, 2H, J = 2.0 Hz), 6.57 (m, 4H), 6.76 (m, 6H), 7.06 (d, 2H, J = 2.0 Hz), 7.37 (m, 2H), 7.39 (d, 2H, J = 2.0 Hz), 7.55 (m, 8H), 7.69 (m, 2H), 7.91 (m, 4H); ^{13}C NMR (125 MHz, CD_2Cl_2, 300 K): δ 119.55, 122.81 (q, $J_{C\text{-}F}$ = 271.5 Hz), 124.74, 125.81, 126.66, 132.58 (qt, $J_{C\text{-}F}$=33.7, $J_{C\text{-}P}$ = 4.6 Hz), 132.87 (2C), 132.98 133.28, 135.02 (t, $J_{C\text{-}P}$ = 13.2 Hz), 135.09 (t, $J_{C\text{-}P}$ = 4.1 Hz), 138.47, 139.88 (t, $J_{C\text{-}P}$ = 33.6 Hz), 141.62; ^{19}F NMR (377 MHz, CD_2Cl_2, 300 K): δ -66.61; ^{31}P {^{1}H} NMR (202 MHz, CD_2Cl_2, 300 K) δ -12.01. Anal. calcd. for $C_{56}H_{32}BCuF_{24}N_4P_2$ (%): C, 49.71; H, 2.38; N, 4.14. Found: C, 49.65; H, 2.21; N, 4.32.

2. NMR Experiments

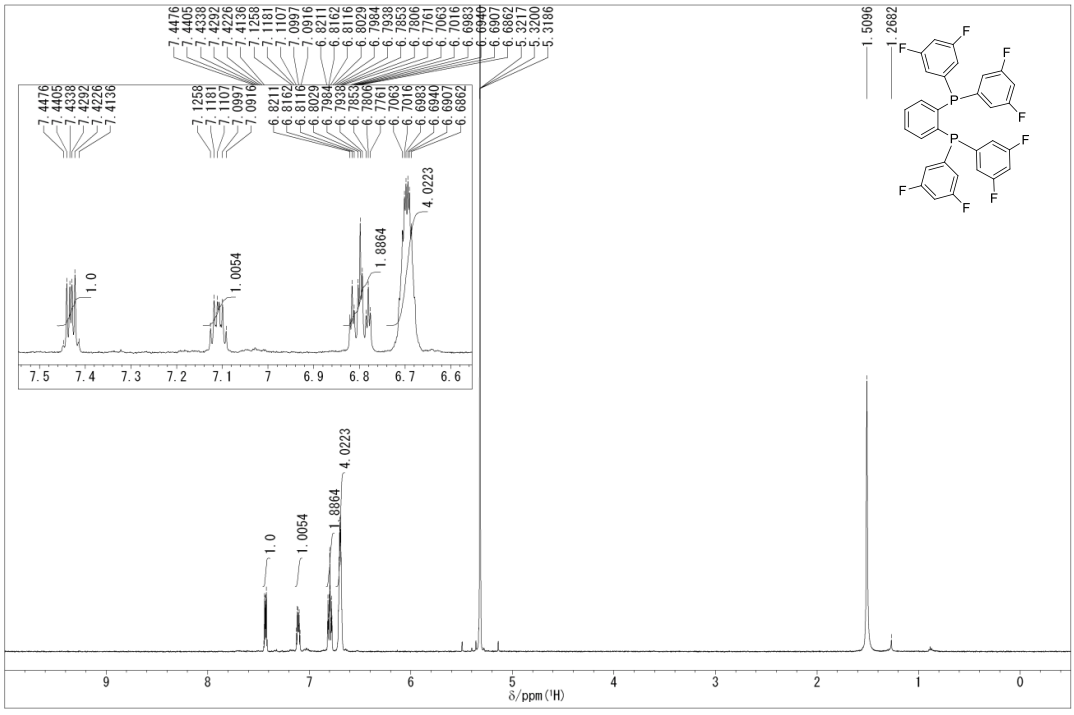

Fig. S1 ^{1}H NMR spectrum of dppb-F in CD_2Cl_2 at 300 K.

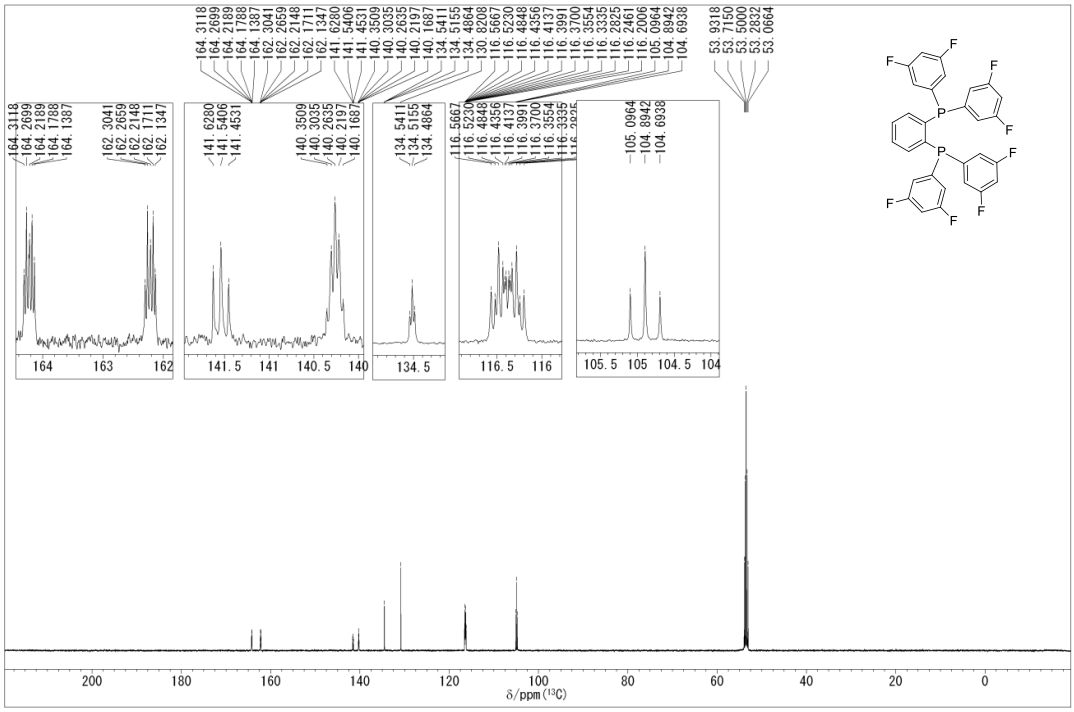

Fig. S2 ^{13}C NMR spectrum of dppb-F in CD_2Cl_2 at 300 K.

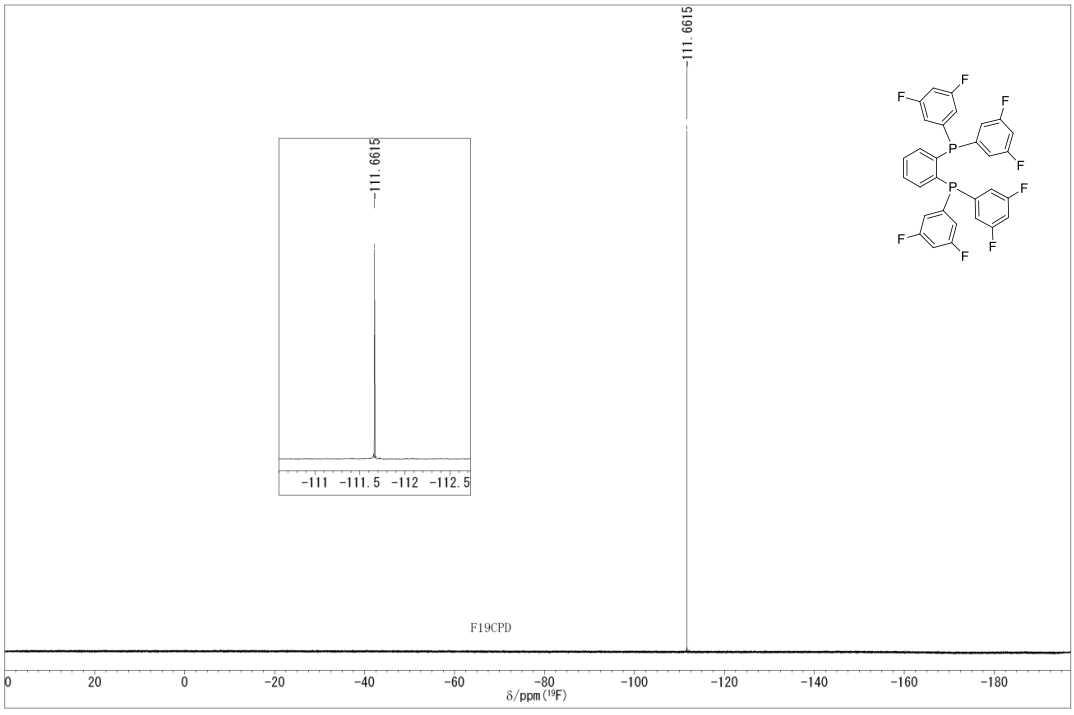

Fig. S3 ^{19}F NMR spectrum of dppb-F in CD_2Cl_2 at 300 K.

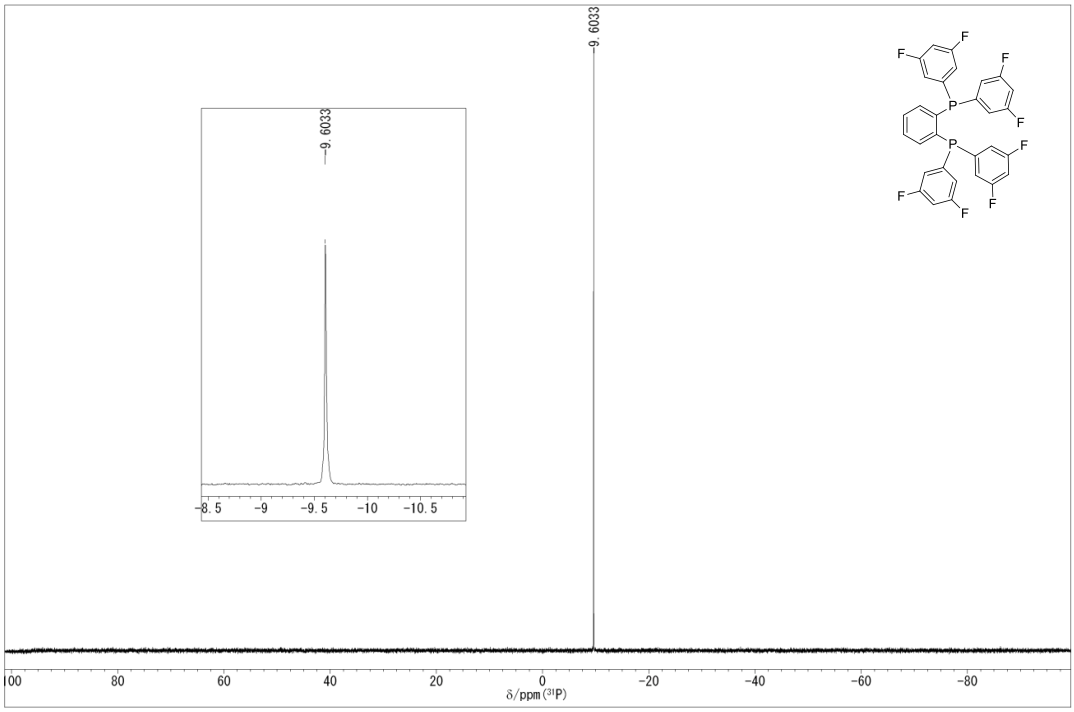

Fig. S4 ^{31}P {^{1}H} NMR spectrum of dppb-F in CD_2Cl_2 at 300 K.

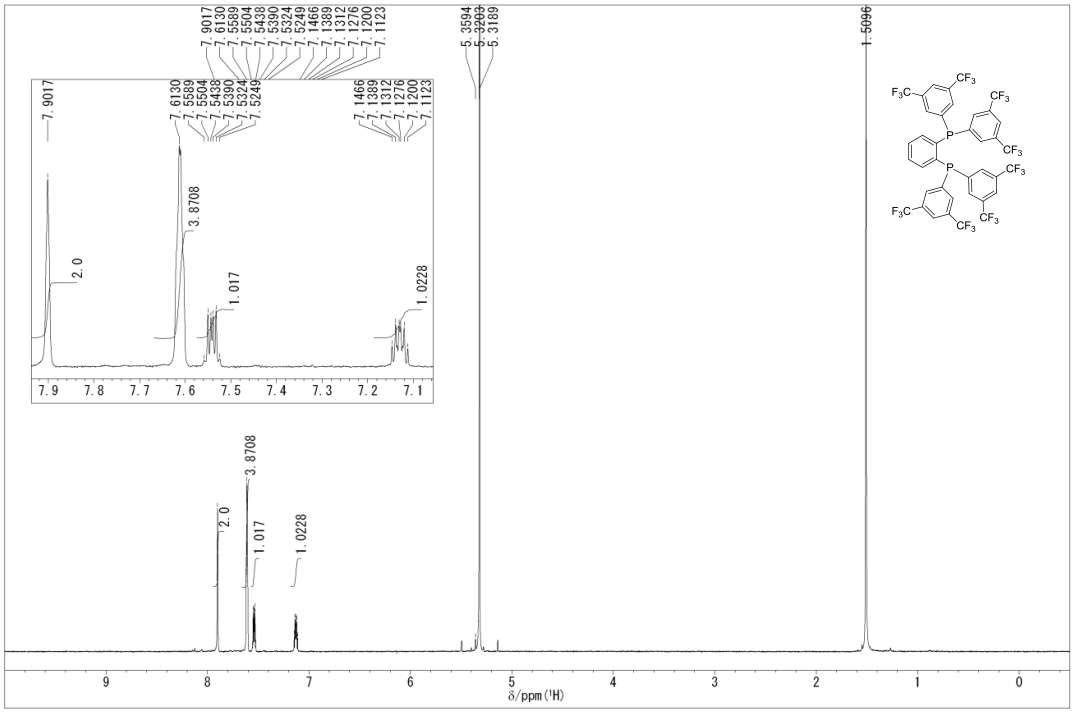

Fig. S5 ^{1}H NMR spectrum of dppb-CF_3 in CD_2Cl_2 at 300 K

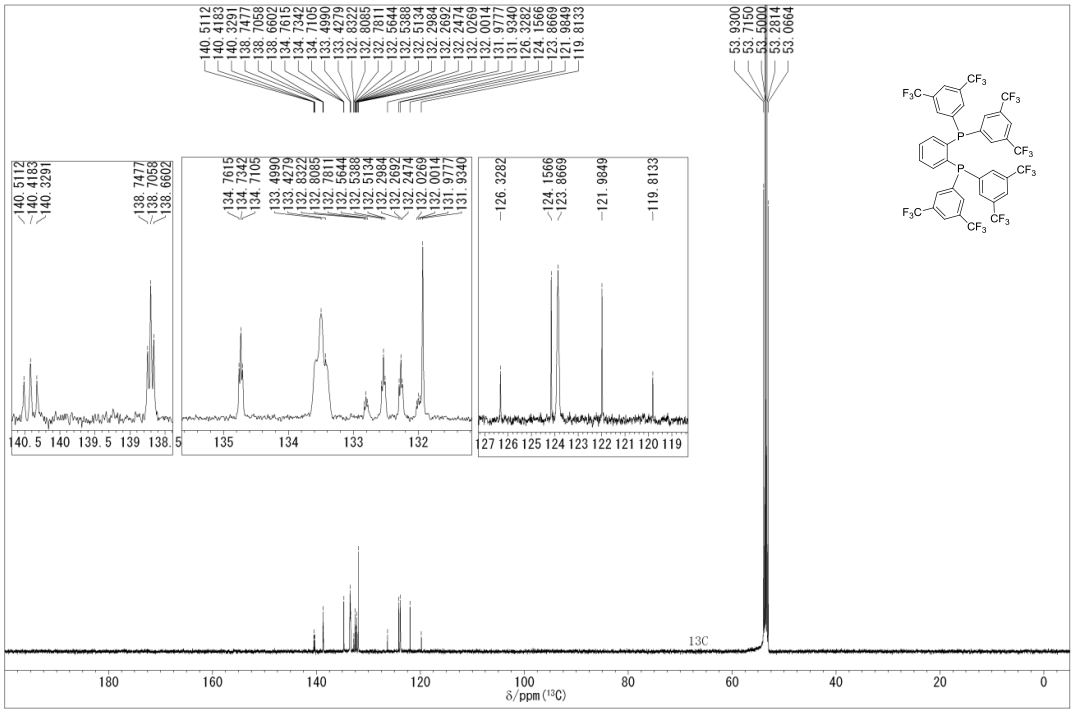

Fig. S6 ^{13}C NMR spectrum of dppb-CF_3 in CD_2Cl_2 at 300 K.

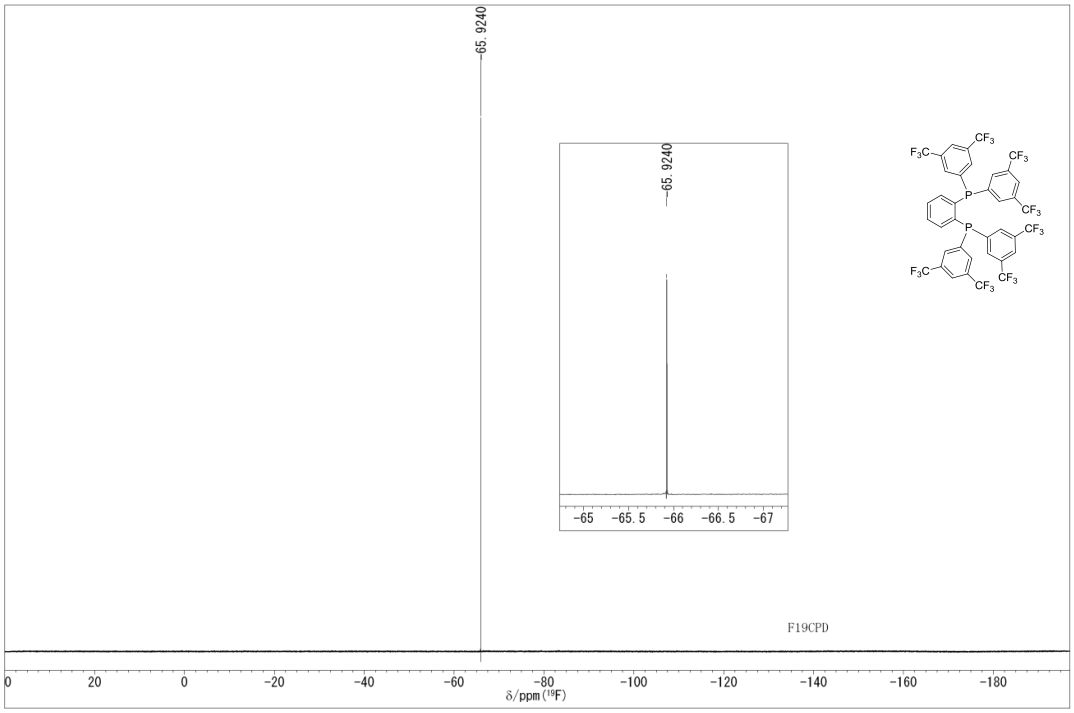

Fig. S7 ^{19}F {^{1}H} NMR spectrum of dppb-CF_3 in CD_2Cl_2 at 300 K.

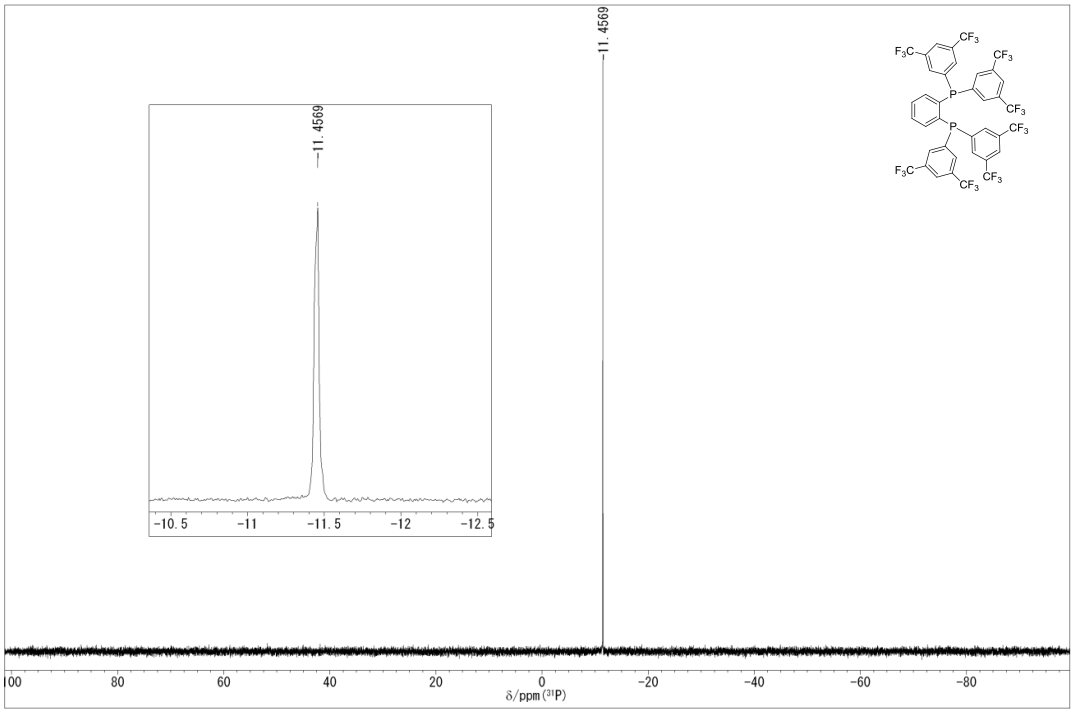

Fig. S8 ^{31}P {^{1}H} NMR spectrum of dppb-CF_3 in CD_2Cl_2 at 300 K.

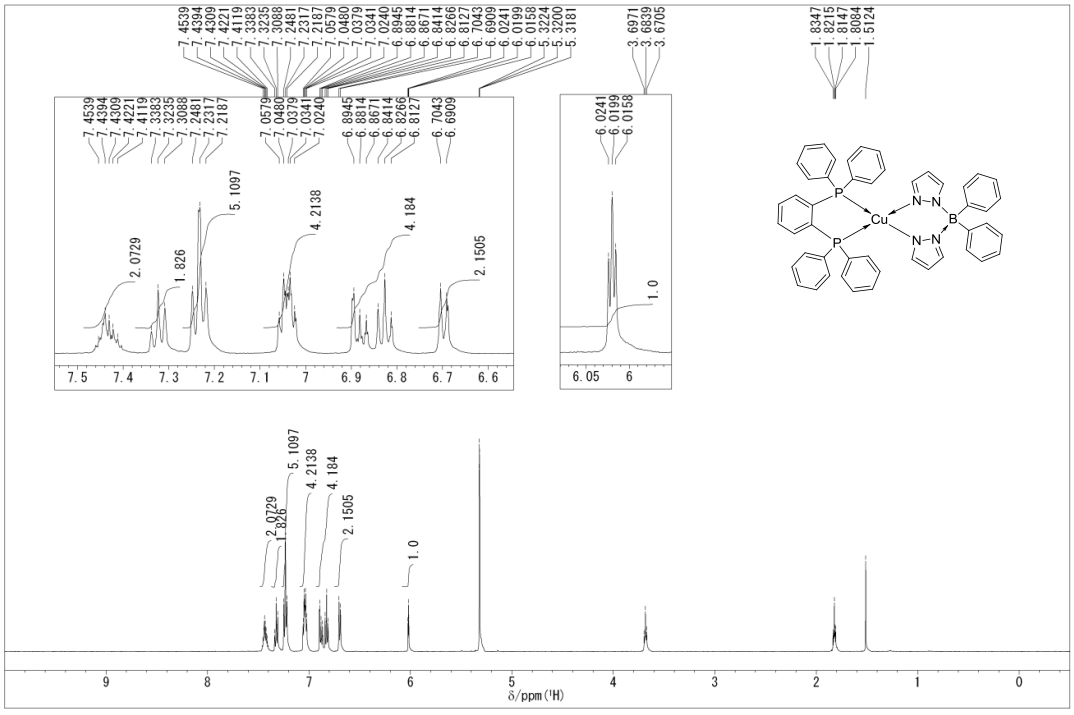

Fig. S9 ^{1}H NMR spectrum of **1** in CD_2Cl_2 at 300 K.

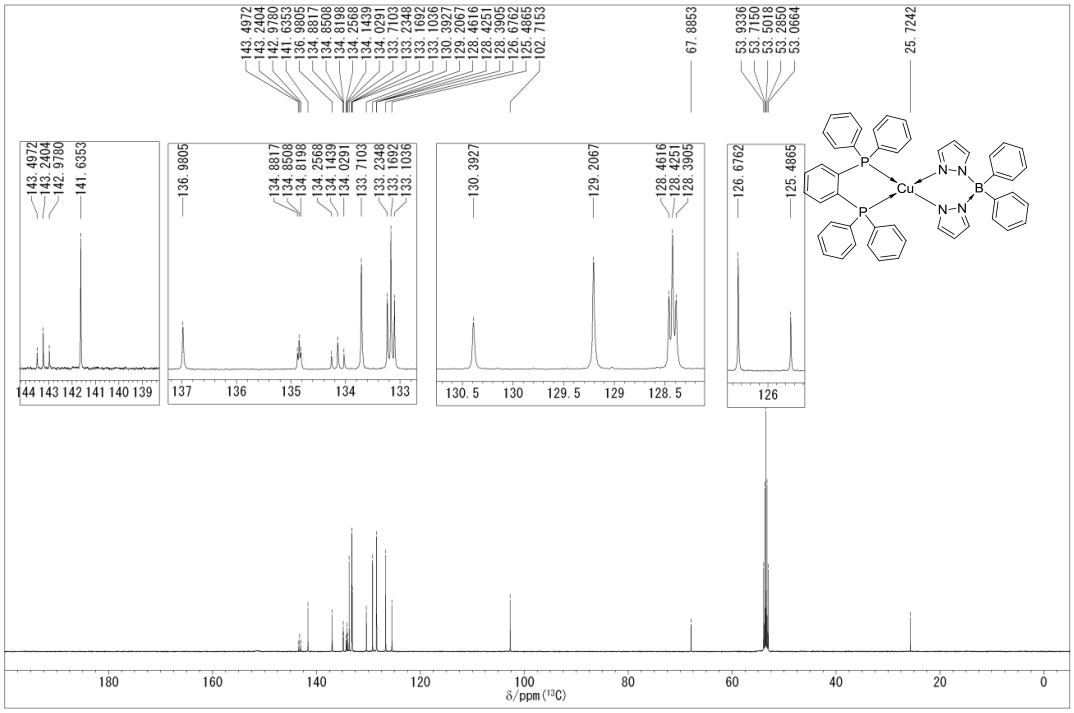

Fig. S10 ^{13}C NMR spectrum of **1** in CD_2Cl_2 at 300 K.

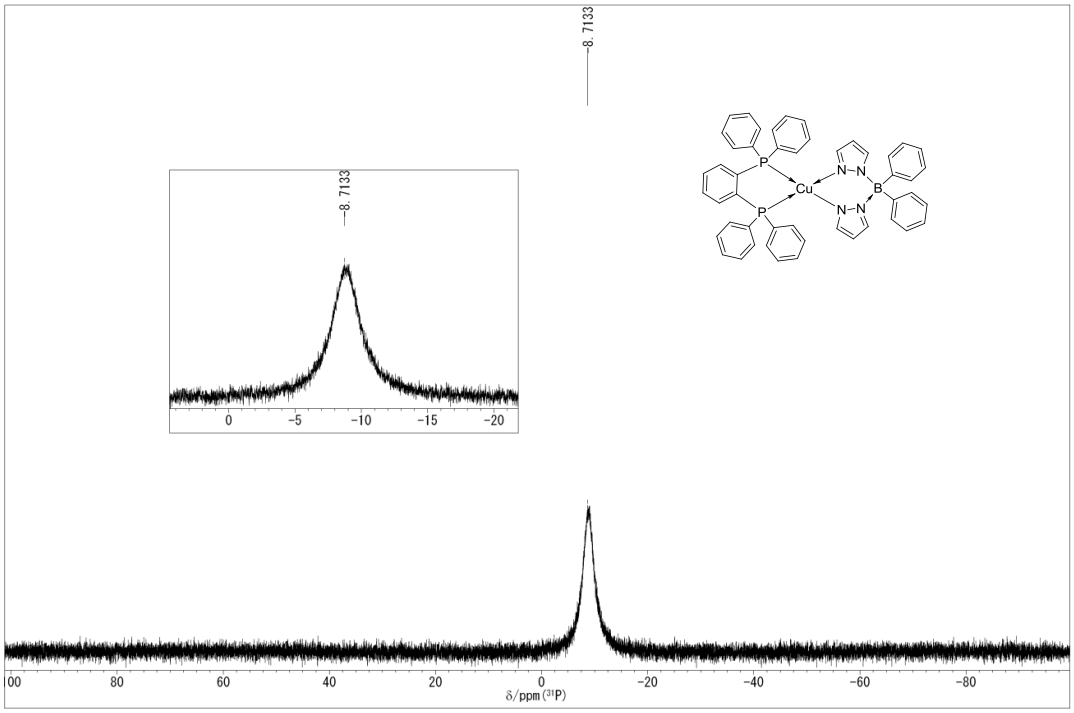

Fig. S11 ^{31}P {^{1}H} NMR spectrum of **1** in CD_2Cl_2 at 300 K.

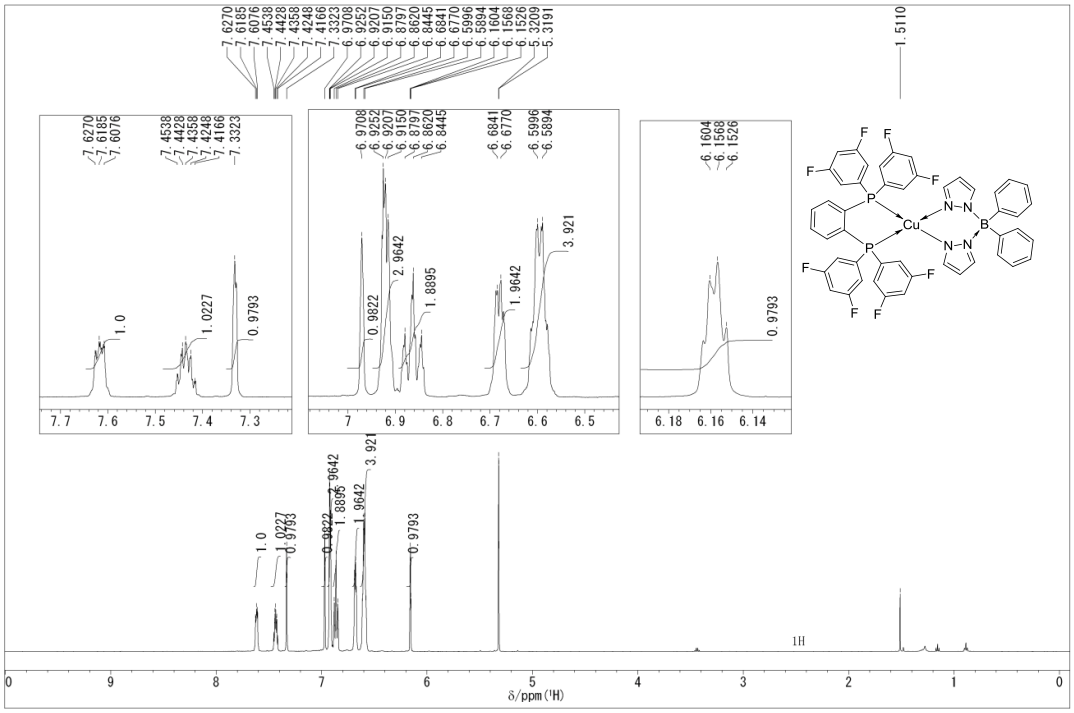

Fig. S12 ^{1}H NMR spectrum of **2** in CD_2Cl_2 at 300 K.

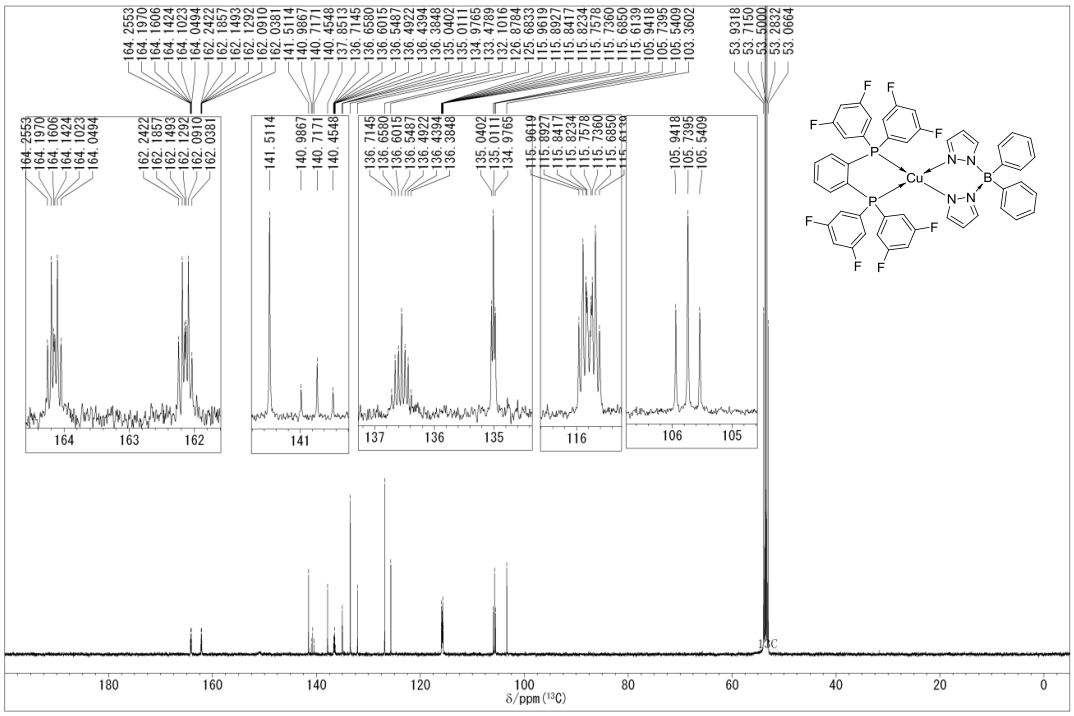

Fig. S13 ^{13}C NMR spectrum of **2** in CD_2Cl_2 at 300 K.

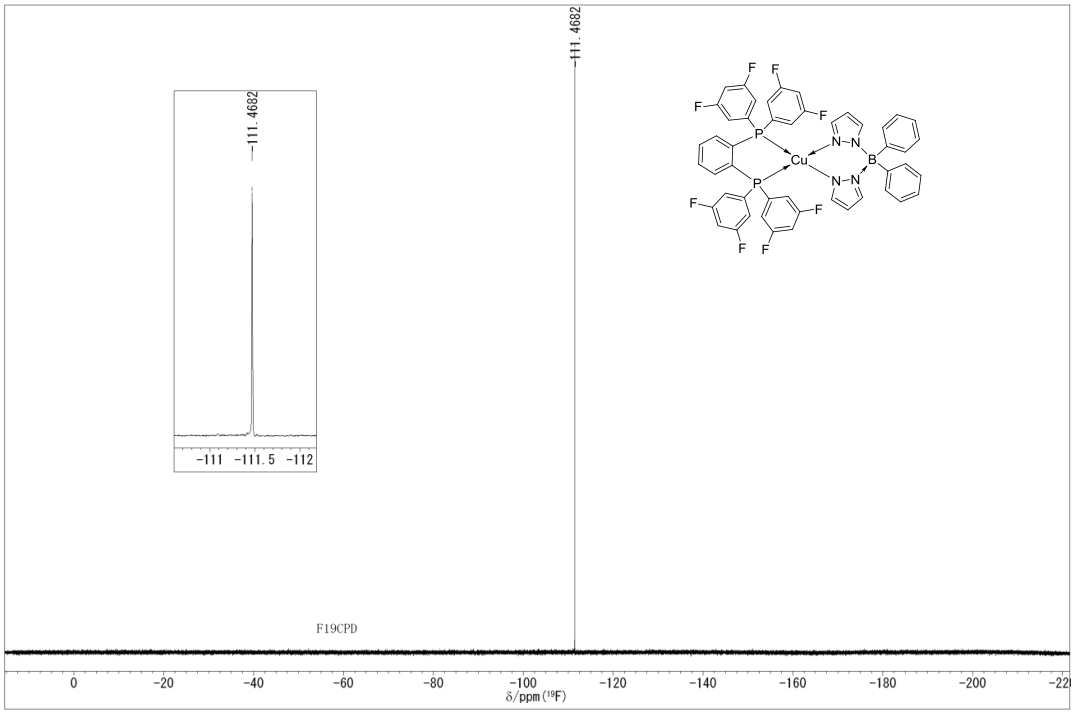

Fig. S14 ^{19}F {^{1}H} NMR spectrum of **2** in CD_2Cl_2 at 300 K.

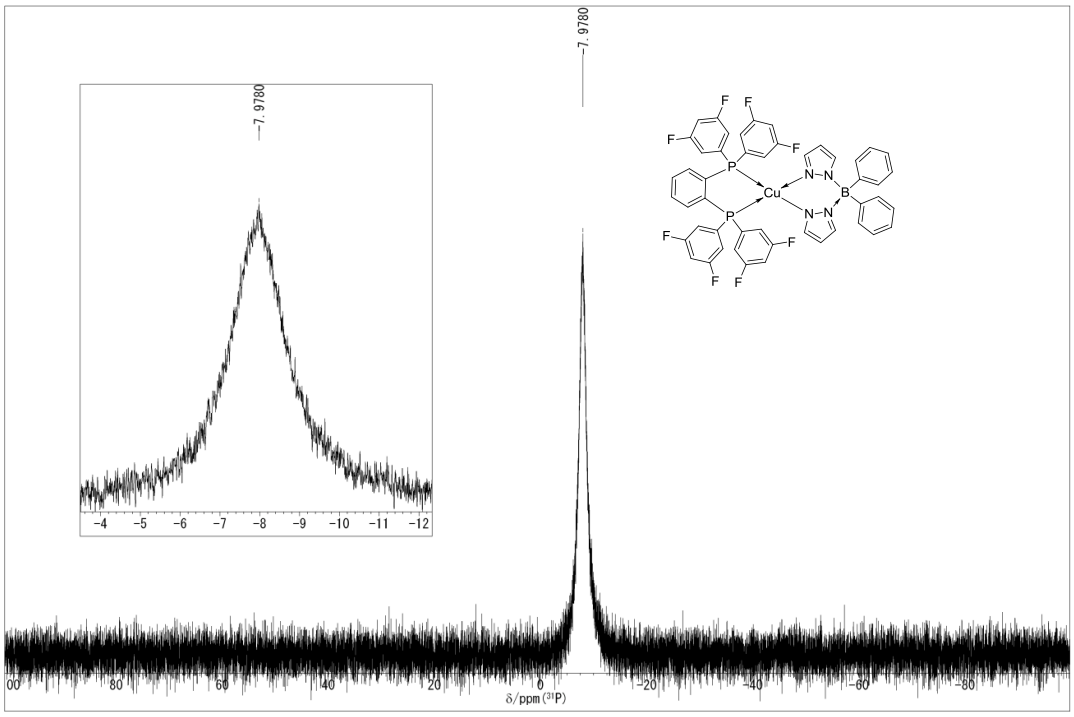

Fig. S15 ^{31}P {^{1}H} NMR spectrum of **2** in CD_2Cl_2 at 300 K.

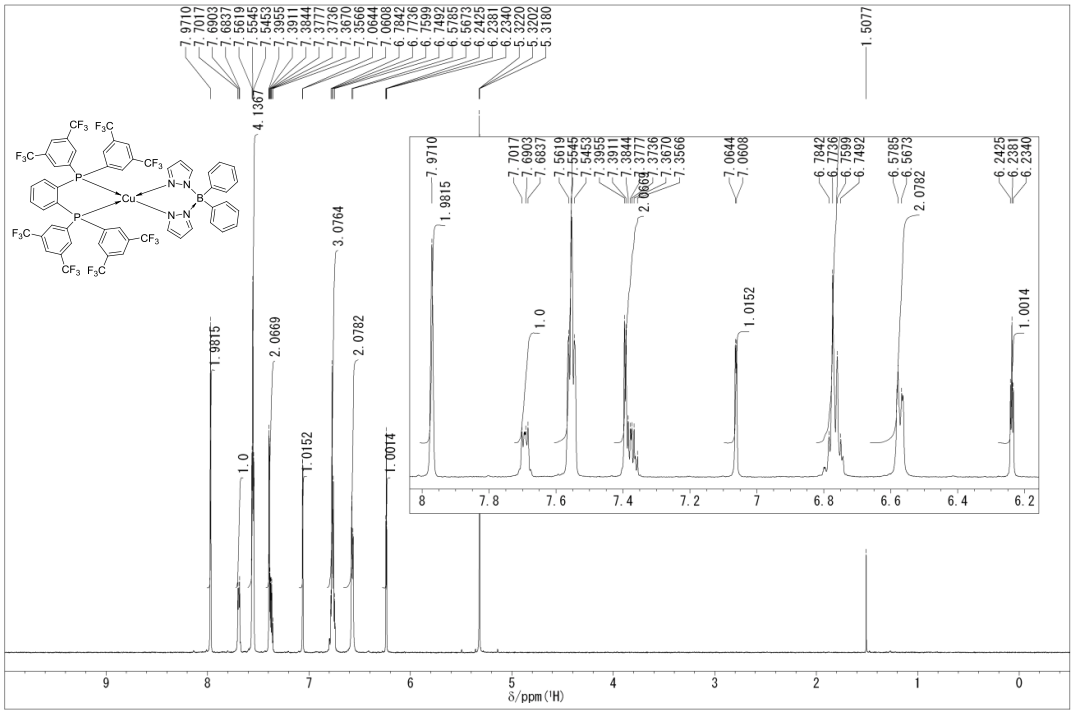

Fig. S16 ^{1}H NMR spectrum of **3** in CD_2Cl_2 at 300 K

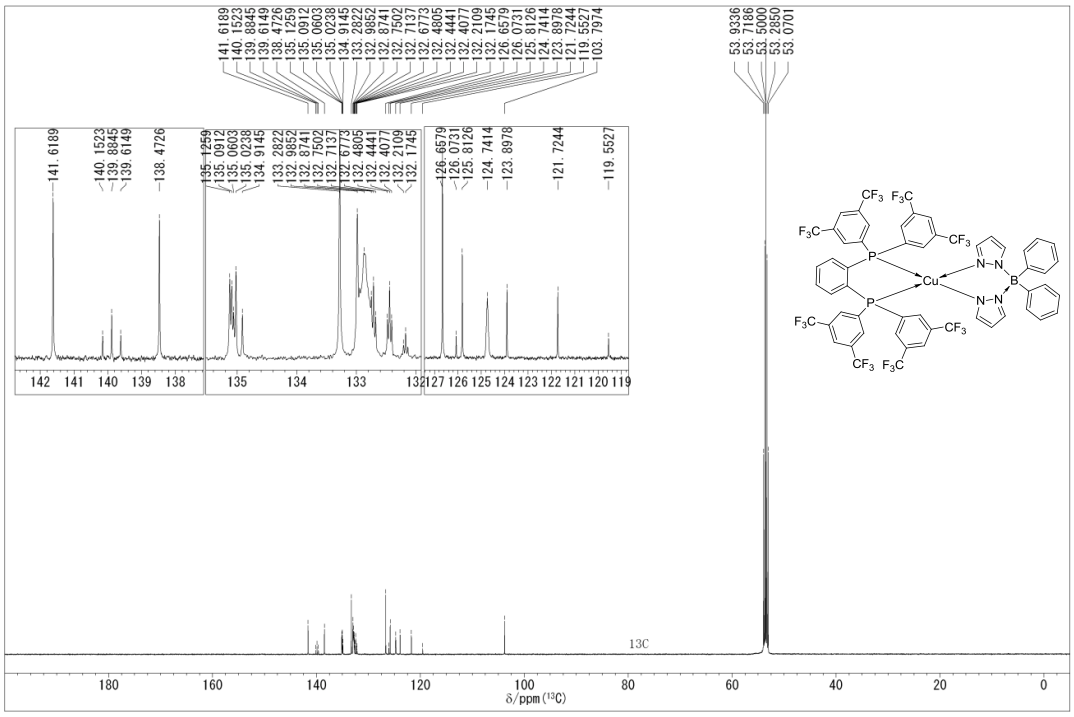

Fig. S17 ^{13}C NMR spectrum of **3** in CD_2Cl_2 at 300 K.

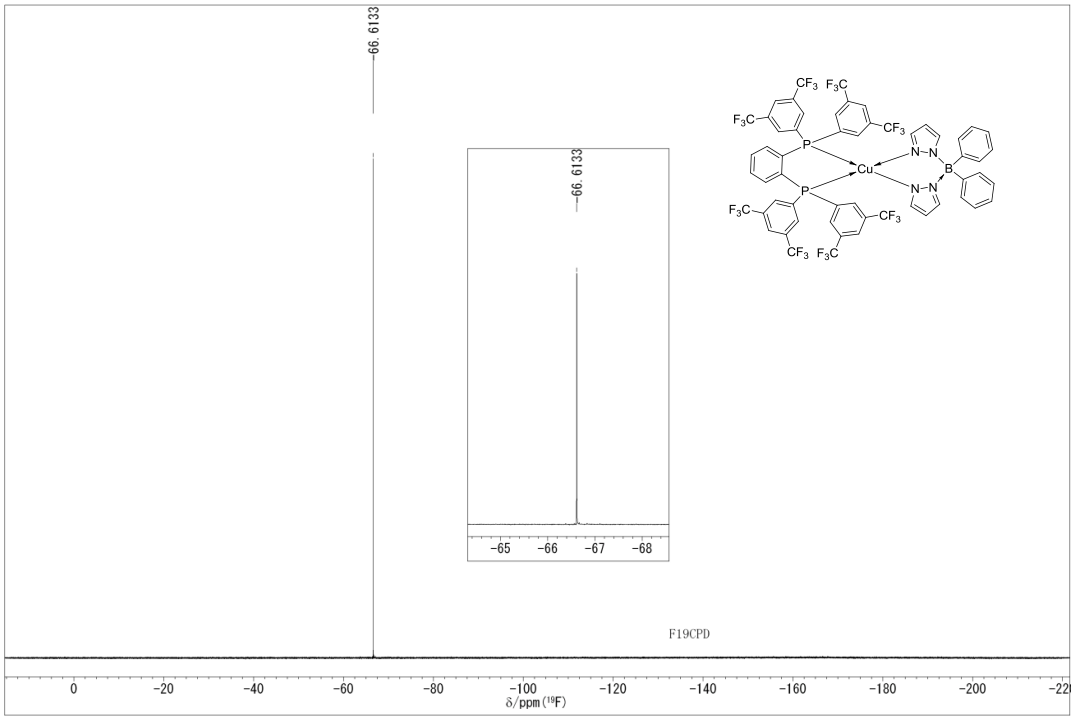

Fig. S18 ^{19}F {^{1}H} NMR spectrum of **3** in CD_2Cl_2 at 300 K.

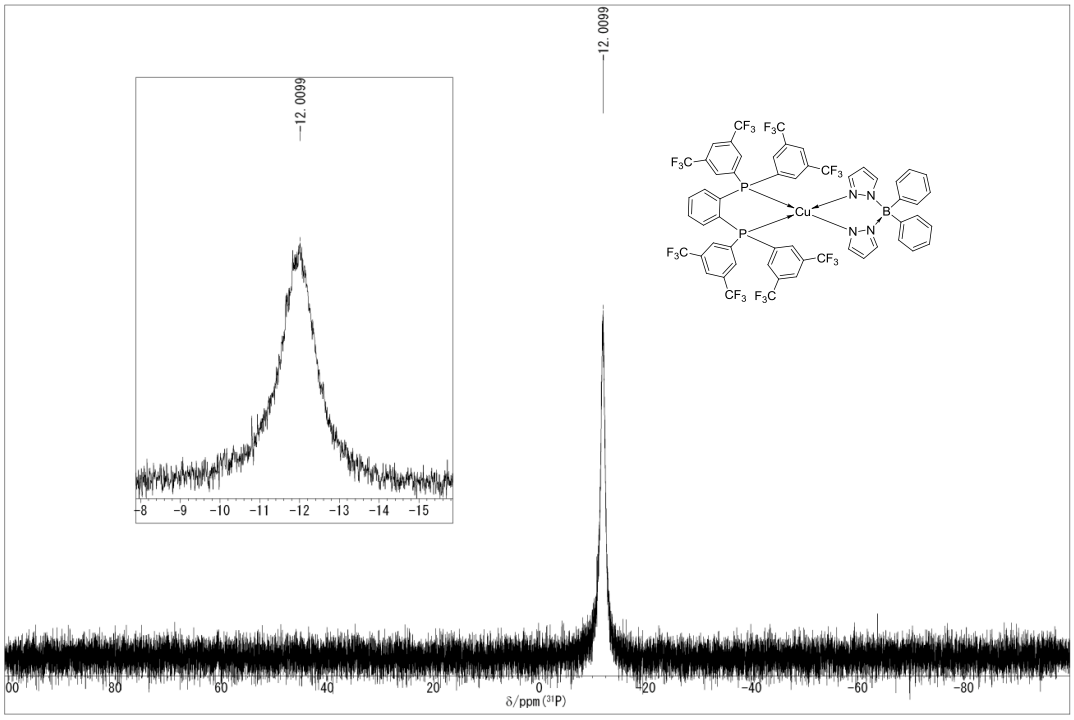

Fig. S19 ^{31}P {^{1}H} NMR spectrum of **3** in CD_2Cl_2 at 300 K.

3. Crystal Structure Determination

Table S1 Crystallographic data for **1−3**

	1	**2**	**3**
formula	$C_{48}H_{40}BCuN_4P_2\ CH_2Cl_2$	$C_{48}H_{32}BCuF_8N_4P_2$	$C_{56}H_{32}BCuF_{24}N_4P_2$
formula weight	894.06	953.07	1353.15
cryst syst	monoclinic	triclinic	orthorhmbic
space group	$P2_1/c$	$P\bar{1}$	*Pbca*
a / Å	9.6512 (8)	12.4467 (2)	12.6861 (16)
b / Å	22.813 (2)	13.2352 (11)	20.390 (3)
c / Å	19.5335 (17)	13.7652 (9)	44.345 (6)
α / deg	-	89.778 (4)	-
β / deg	93.960 (2)	70.725 (4)	-
γ / deg	-	78.648(3)	-
V / Å^3	4290.4(6)	2094.0(3)	11471(2)
Z	4	2	8
d_{calcd} / g cm^{-3}	1.384	1.512	1.567
T / K	90.0(1)	90.0(1)	90.0(1)
radiation	Mo Kα	Mo Kα	Mo Kα
	(λ = 0.71073 Å)	(λ = 0.71073 Å)	(λ = 0.71073 Å)
μ / cm^{-1}	0.749	0.675	0.557
diffractometer	Rigaku AFC-8	Rigaku AFC-8	Rigaku AFC-8
max 2θ / deg	60	60	60
reflns collcd	115869	29243	75702
indep reflns	13634	12050	16699
	(*R*int = 0.061)	(*R*int = 0.023)	(*R*int = 0.0755)
no. of param refined	574	7578	820
R1, *wR2* ($I > 2\sigma I$)	0.0677, 0.1658	0.0297, 0.0802	0.0671, 0.1561
S	1.120	1.087	1.132

4. Cyclic Voltammagram Measurement

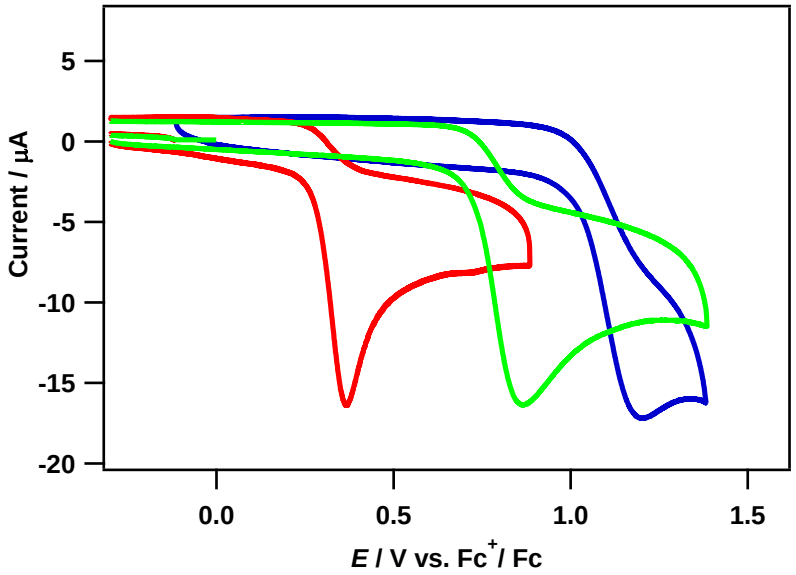

Fig. S20 Cyclic voltammagram of dppb (red), dppb-F (green), and dppb-CF_3 (blue) in CH_3CN at 293 K.

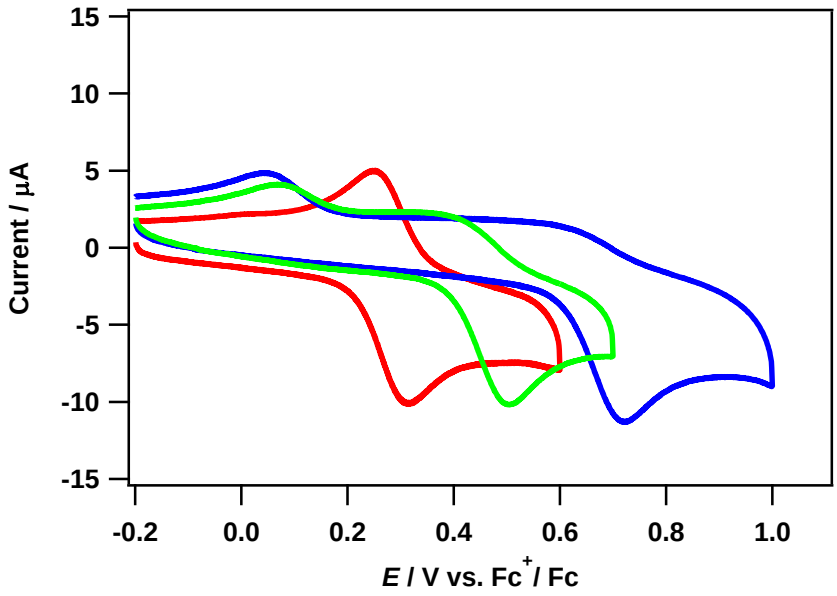

Fig. S21 Cyclic voltammagram of **1** (red), **2** (green), and **3** (blue) in CH_3CN at 293 K.

5. Theoretical Studies

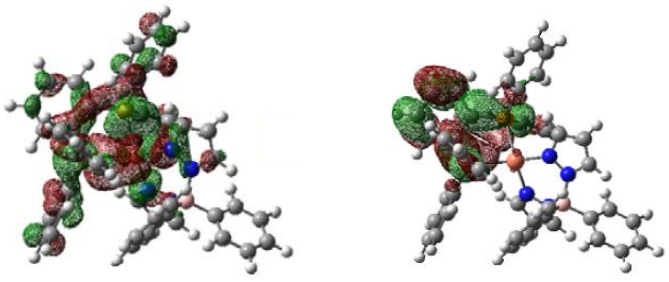

hole **electron**

Fig. S22 NTO pairs for the lowest triplet excited state of **1** in the optimized T_1 geometry. The generation probabilities are 99.5 %.

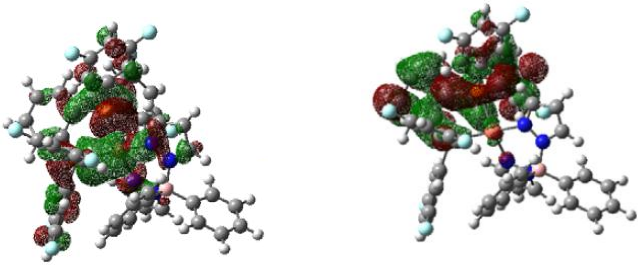

hole electron

Fig. S23 NTO pairs for the lowest triplet excited state of **2** in the optimized T_1 geometry. The generation probabilities are 99.7 %.

Table S2. Compositions of hole and electron in T_1 of **3** (the optimized T_1 geometry in THF)

	percentage composition (%) [a]		
	hole	electron	differences
Cu	38.4	0.64	37.8
P1	13.6	1.06	12.5
P2	15.1	7.00	8.08
N1	6.21	0.06	6.15
N3	6.55	0.03	6.52
P and N (total)	41.5	8.15	33.4
others	20.1	91.2	-71.1

[a] In the molecular orbitals, the atomic component is evaluated by the sum of the square of the LCAO coeffiients which belong to the corresponding atom; see experimental section in detail.

Table S3. Compositions of hole and electron in T_1 of **1**. (the optimized T_1 geometry in THF)

	percentage composition (%) [a]		
	hole	electron	differences
Cu	34.5	0.587	33.9
P1	15.2	3.58	11.6
P2	16.7	2.67	14.0
N1	4.87	0.06	4.81
N3	4.37	0.02	4.35
P and N (total)	41.1	6.33	35.1
others	24.4	93.1	-67.7

[a] In the molecular orbitals, the atomic component is evaluated by the sum of the square of the LCAO coeffiients which belong to the corresponding atom; see experimental section in detail.

Table S4. Compositions of hole and electron in T_1 of **2**. (the optimized T_1 geometry in THF)

	percentage composition (%) [a]		
	hole	electron	differences
Cu	38.9	1.08	37.8
P1	13.3	9.07	4.19
P2	15.8	0.95	14.9
N1	6.02	0.20	5.82
N3	5.69	0.027	5.66
P and N (total)	40.8	10.3	30.5
others	20.3	89.7	-69.4

[a] In the molecular orbitals, the atomic component is evaluated by the sum of the square of the LCAO coeffiients which belong to the corresponding atom; see experimental section in detail.

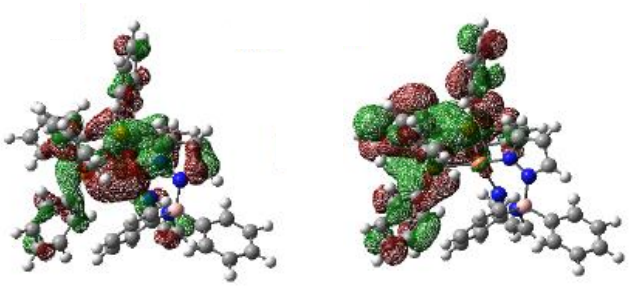

hole **electron**

Fig. S24 NTO pairs for the lowest triplet excited state of **1** in the optimized S_0 geometry. The generation probabilities are 94.4 %.

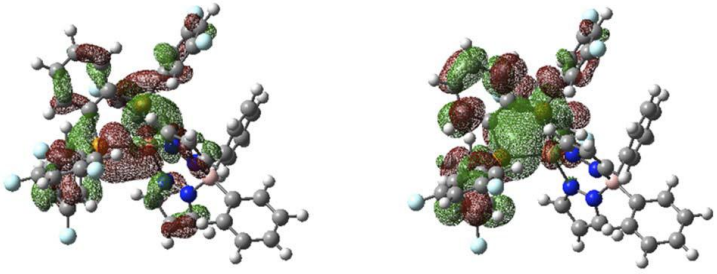

hole **electron**

Fig. S25 NTO pairs for the lowest triplet excited state of **2** in the optimized S_0 geometry. The generation probabilities are 93.4 %.

Table S5 Compositions of hole and electron in T_1 of **3** (optimized S_0 geometry in THF)

	percentage composition (%) [a]		
	hole	electron	differences
Cu	30.2	0.97	29.3
P1	14.3	4.76	9.57
P2	15.6	2.03	13.6
N1	3.71	0.20	3.51
N3	2.70	0.082	2.62
P and N (total)	40.8	10.3	30.5
Others	29.0	88.7	-59.7

[a] In the molecular orbitals, the atomic component is evaluated by the sum of the square of the LCAO coeffiients which belong to the corresponding atom; see experimental section in detail.

Table S6 Compositions of hole and electron in T_1 of **1** (optimized S_0 geometry in THF)

	percentage composition (%) [a]		
	hole	electron	differences
Cu	28.6	0.65	28.0
P1	16.6	3.90	12.7
P2	17.6	2.59	15.0
N1	1.29	0.10	1.19
N3	1.64	0.072	1.57
P and N (total)	37.1	6.66	30.4
Others	34.3	92.7	-58.4

[a] In the molecular orbitals, the atomic component is evaluated by the sum of the square of the LCAO coeffiients which belong to the corresponding atom; see experimental section in detail.

Table S7 Compositions of hole and electron in T_1 of **2** (optimized S_0 geometry in THF)

	percentage composition (%) [a]		
	hole	electron	differences
Cu	31.0	1.66	29.3
P1	15.0	6.65	8.35
P2	15.7	5.42	10.3
N1	2.29	0.40	1.90
N3	2.60	0.097	2.50
P and N (total)	35.6	14.23	21.4
Others	33.4	91.7	-58.3

[a] In the molecular orbitals, the atomic component is evaluated by the sum of the square of the LCAO coeffiients which belong to the corresponding atom; see experimental section in detail.

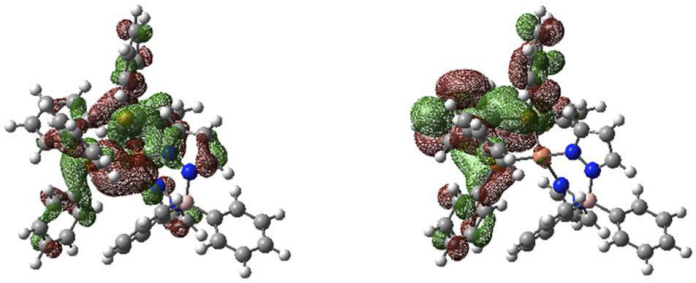

hole **electron**

Fig. S26 NTO pairs for the first singlet excited state of **1** in the optimized S_0 geometry. The generation probabilities are 99.9 %.

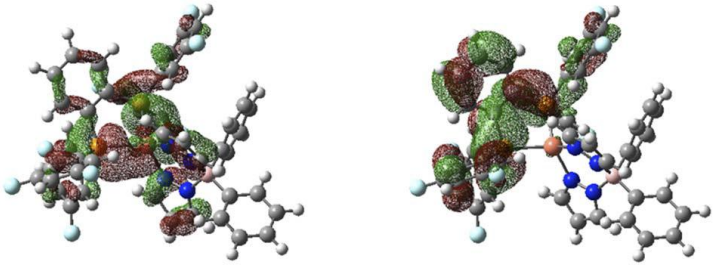

hole **electron**

Fig. S27 NTO pairs for the first singlet excited state of **2** in the optimized S_0 geometry. The generation probabilities are 99.8 %.

Table S8 Compositions of hole and electron in S_1 of **3** (optimized S_0 geometry in THF)

	percentage composition (%) [a]		
	hole	electron	differences
Cu	31.9	1.00	30.9
P1	15.7	5.38	10.3
P2	17.2	1.46	15.8
N1	3.80	0.22	3.57
N3	2.81	0.075	2.74
P and N (total)	39.5	6.66	32.8
others	28.6	92.3	-63.7

[a] In the molecular orbitals, the atomic component is evaluated by the sum of the square of the LCAO coeffiients which belong to the corresponding atom; see experimental section in detail.

Table S9 Compositions of hole and electron in S_1 of **1** (optimized S_0 geometry in THF)

	percentage composition (%) [a]		
	hole	electron	differences
Cu	30.5	0.23	30.3
P1	18.8	3.89	14.9
P2	19.9	1.62	18.3
N1	1.21	0.26	1.18
N3	1.61	0.017	1.60
P and N (total)	41.5	6.02	35.5
others	28.0	93.8	-65.8

[a] In the molecular orbitals, the atomic component is evaluated by the sum of the square of the LCAO coeffiients which belong to the corresponding atom; see experimental section in detail.

Table S10 Compositions of hole and electron in S_1 of **2** (optimized S_0 geometry in THF)

	percentage composition (%) [a]		
	hole	electron	differences
Cu	33.1	0.18	33.0
P1	17.3	4.33	13.0
P2	18.2	2.51	15.7
N1	2.24	0.01	2.23
N3	2.68	0.00	2.68
P and N (total)	40.4	6.02	35.5
others	26.5	93.8	-67.3

[a] In the molecular orbitals, the atomic component is evaluated by the sum of the square of the LCAO coeffiients which belong to the corresponding atom; see experimental section in detail.

6. The angular distribution of light emission from OLEDs containing 1 – 3.

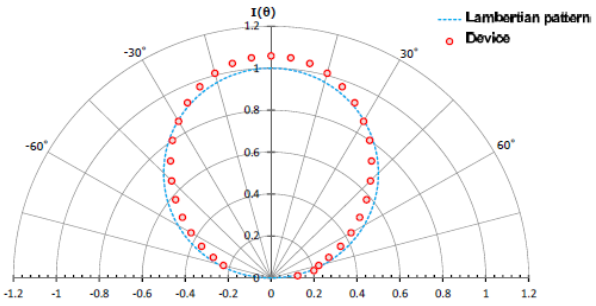

Fig. S28 The angular distribution of light emission from the device containing **1**.

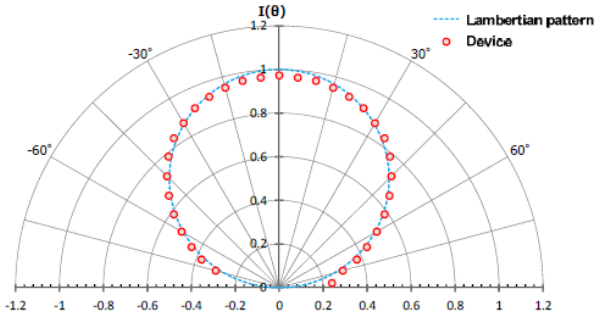

Fig. S29 The angular distribution of light emission from the device containing **2**.

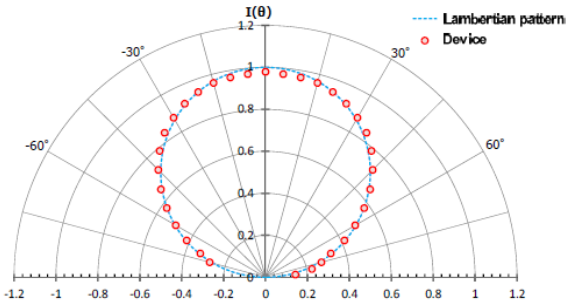

Fig. S30 The angular distribution of light emission from the device containing **3**.

7. References

1. W. J. Layton, K. Niedenzu, P. M. Niedenzu and S. Trofimenko, *Inorganic Chemistry*, 1985, **24**, 1454-1457.
2. A. Tsuboyama, K. Kuge, M. Furugori, S. Okada, M. Hoshino and K. Ueno, *Inorganic Chemistry*, 2007, **46**, 1992-2001.